Waste Management 140 (2022) 100–109

Contents lists available at ScienceDirect

Waste Management

journal homepage: www.elsevier.com/locate/wasman

Energy recovery from garden and park waste by hydrothermal carbonisation and anaerobic digestion

R.P. Ipiales [a,b], A.F. Mohedano [a], E. Diaz [a], M.A. de la Rubia [a,*]

[a] Chemical Engineering Department, Universidad Autónoma de Madrid, 28049 Madrid, Spain
[b] Arquimea-Agrotech, 28400 Collado Villalba, Madrid, Spain

ARTICLE INFO

Keywords:
Anaerobic digestion
Circular economy
Energy recovery
Hydrochar
Hydrothermal carbonisation
Process water
Garden and park waste

ABSTRACT

Hydrothermal carbonisation (HTC) can transform wet lignocellulosic biomass, which is not considered an effective biofuel for energy production at the industrial level, into a carbonaceous product called hydrochar (HC) that is suitable for combustion and a process water (PW). PW is an interesting by-product that can be valorised for biogas production via anaerobic digestion (AD). This study presents a new approach for the valorisation of garden and park wastes (GPW) by integrating HTC to generate HC for energy production, while PW is subjected to AD for biogas production. The hydrothermal treatment was performed at 180, 210, and 230 °C, yielding HC with improved physicochemical properties, such as an elevated higher heating value (21–25 MJ kg^{-1}); low ash (<5 wt.%), nitrogen (1.3 wt.%), and sulphur (0.2 wt.%) contents; better fuel ratio (0.4–0.6); and a broad comprehensive combustibility index (8.0×10^{-7} to 9.6×10^{-7} min^{-2} $°C^{-3}$). AD of the generated PW was conducted under mesophilic conditions (35 °C), resulting in a methane production in the range of 253–326 mL g^{-1} COD_{added} and COD removal of up to 65%. The combination of HTC and AD allowed the recovery of 91% and 94% of the energy content feedstock, as calculated from the combustion of HC and methane, respectively.

1. Introduction

Household waste as well as garden and park waste (GPW), technically known as bio-waste, account for a significant part of municipal solid waste. In 2018, ~2.49×10^8 t of municipal solid waste was generated in the European Union (EU), among which food waste and GPW accounted for ~8.6×10^7 t and 3.6×10^7 t, respectively (EUROSTAT, 2019). GPW is mainly managed by composting and other recycling methods (up to 47%), followed by energy recovery (28%) and landfilling (up to 25%) (EUROSTAT, 2019). GPW has a complex structure (mainly hemicellulose (20–35 wt.%), cellulose (35–50 wt.%), and lignin (10–25 wt.%)), which makes it resistant to microbial degradation. Thus, the composting process takes a long time (4–8 weeks) and requires large areas, resulting in a very low value-added product (Liu et al., 2013). Apart from composting, GPW can be subjected to anaerobic digestion (AD) as another biological option. However, during the digestion of these materials, process inhibition or low biogas production usually occurs owing to the structural complexity of GPW, as mentioned above (Antero et al., 2020). Consequently, treatment of GPW prior to AD (pretreatment) is necessary to achieve a higher biogas yield.

As another approach, the direct disposal of GPW in landfills generates approximately 136 kg CO_2 t^{-1} GPW, whereas incineration produces 71.3 kg CO_2 t^{-1} GPW (Araújo et al., 2018). Thus, these treatments cannot be considered as environmentally friendly processes in the management of these wastes. GPW, one of the most abundant energy resources on the planet, cannot be considered an ideal fuel at the industrial level because of its fibrous nature, low bulk density, and calorific value, as well as high moisture, volatile matter (VM), and ash contents. Moreover, although GPW produces low SO_x and NO_x emissions (Yang et al., 2016), its direct combustion or co-combustion with coal is highly problematic because of the extreme difference in mass and energy density, which results in a lower combustion temperature, higher CO emissions, and corrosion, fouling, and sintering in the combustion equipment (Kambo and Dutta, 2015).

Thermochemical processes such as gasification, liquefaction, pyrolysis, torrefaction, and hydrothermal carbonisation (HTC) are prospectively more advantageous than biological processes for the valorisation of lignocellulosic biomass such as GPW (Wang et al., 2019c). The main products of these thermal processes are syngas (gasification), biofuel (liquefaction), biochar (torrefaction), biofuel and/or biochar (pyrolysis), and hydrochar (HTC), which usually exhibit better physical and chemical properties than those of the feedstock to be used as alternative

* Corresponding author.
E-mail address: angeles.delarubia@uam.es (M.A. de la Rubia).

https://doi.org/10.1016/j.wasman.2022.01.003
Received 4 August 2021; Received in revised form 23 December 2021; Accepted 7 January 2022
Available online 22 January 2022

fuels. HTC uses water as the reaction medium, thereby proving suitable for treating wet biomass without pre-drying (which is mandatory for pyrolysis and gasification); it is implemented at mild temperatures (180–250 °C), relatively short residence times (5–240 min), and self-generated pressure (2–6 MPa) (Kambo and Dutta, 2015; Villamil et al., 2020a; Zhang et al., 2017). The main products of HTC are a solid fraction called hydrochar (HC), a liquid fraction generally termed process water (PW), and a gaseous phase composed mainly of CO_2.

The HC obtained is rich in carbon, it contains approximately 41–85 wt.% of the initial carbon and has 50–85% of the energy contained in the feedstock (Fang et al., 2018; Ipiales et al., 2021). It also exhibits better physicochemical properties than those of feedstock, such as a homogeneous chemical composition, high higher heating value (HHV), high energy density (Ischia and Fiori, 2020), and lower nitrogen, sulphur, and ash contents; therefore, it is an alternative biofuel (Aragón-Briceño et al., 2021; Marin-Batista et al., 2020b). The combustion of these HCs could produce lower NOx and SOx emissions. During HTC, most of the alkali metals are transferred to the PW, which improves the combustion characteristics of HCs and reduces slag formation and fouling (Wang et al., 2019a). Some researchers have observed that metal accumulation in HC can cause adverse problems during combustion, especially when sewage sludge, animal manure, or algae are used (Aragón-Briceño et al., 2020; Lentz et al., 2019; Marin-Batista et al., 2019). However, lignocellulosic biomass, owing to its relatively low ash content, shows an opposite trend (Lucian et al., 2019). Thus, proper feedstock selection and suitable HTC operating conditions can help reduce these problems (Ipiales et al., 2021; Reza et al., 2013). Furthermore, according to Medina-Martos et al. (2020), HC combustion emits less greenhouse gases (18 kg CO_2 equiv t^{-1} of HC) than those produced via direct combustion of GPW or sewage sludge (similar in both cases: ≈ 72 kg CO_2 equiv t^{-1}).

Furthermore, HCs can be used as soil amendments (Bargmann et al., 2014; Islam et al., 2021), sorbents for CO_2 sequestration, and precursors for the preparation of activated carbon, while being applicable in energy storage devices (Li/Na ion batteries, supercapacitors, fuel cells, etc.) (Diaz et al., 2019; Islam et al., 2021; Schonvogel et al., 2019). The aqueous fraction resulting from the hydrothermal process is a by-product with an interesting valorisation potential, as it contains a high content of organic matter, nutrients, and minerals. Particular attention has been paid to the recovery of phosphorus, which can be precipitated into struvite for use as a fertiliser (Marin-Batista et al., 2020a). Furthermore, the possibility of recirculating PW facilitates the increase in carbon recovery yield, while augmenting the energy density of the HC (Picone et al., 2021). Treatment of PW via AD (Ahmed et al., 2021; Gaur et al., 2020), aerobic oxidation (Langone et al., 2021; Weide et al., 2019), or wet air oxidation (Reza et al., 2016) has also been considered.

The synergy between HTC and AD optimises the energy efficiency of the process, especially in the case of low-quality waste, such as sewage sludge or animal manure (Bardhan et al., 2021). However, improving the energy efficiency of HTC and AD is highly dependent on the quality of the initial feedstock and operational conditions, such as temperature, reaction time, and biomass/water ratio (Ipiales et al., 2021). A low temperature (<200 °C), short reaction time (≤60 min), and high biomass/water ratio have been reported to achieve high energy efficiency by maximising HC yield and PW biodegradability under anaerobic conditions (Gaur et al., 2020; Lucian et al., 2020; Wang et al., 2022).

This study investigates the synergy between a thermochemical process (such as HTC) and a biological process (such as AD), for the purpose of valorising lignocellulosic biomass (GPW) to obtain biofuels (HC and biogas). This combined approach aims to improve the energy efficiency of the HTC process by valorising PW for biogas production and increasing the energy efficiency of the overall process.

2. Materials and methods

2.1. Feedstock origin

GPW was collected from the Migas Calientes Composting Plant located in Madrid, Spain. Plant-based waste was collected from public gardens in Madrid, Spain. The feedstock was ground and sieved to reduce and homogenise the particle size (<3 mm). The ground feedstock was then stored in closed containers at room temperature until the HTC experiments were performed.

2.2. Hydrothermal carbonisation and anaerobic digestion experiments

The HTC experiments were performed in an electrically heated 4 L ZipperClave® pressure vessel. GPW has a very low moisture content (~5%); therefore, it was mixed with deionised water (DW) (20:80 (w:w)). A 1.2 kg sample of the substrate (GPW+DW) was treated at three temperatures (180, 210, and 230 °C), with a heating ramp of 3 °C min^{-1} and holding time of 1 h. The reaction was stopped by cooling with an internal heat exchanger using tap water. The obtained suspension was then centrifuged in a SIGMA 3-16L centrifuge equipped with a fixed-angle rotor (cod. 12159). The HC was oven-dried to a constant weight, and then ground and sieved using a Filtra No. 38,373 sieve. Subsequently, the smallest fraction (<0.25 mm) was characterised. The PW was recovered by filtration (0.45 mm) and maintained at 4 °C for use as a substrate in the AD process. The HC samples are denoted as HC180, HC210, and HC230, while the PW samples are represented as PW180, PW210, and PW230; here, the numbers correspond to the HTC temperatures. The HTC experiments were performed in duplicate.

AD cycles were performed in 120 mL glass serum flasks. The inoculum used in the anaerobic batch tests was a granular anaerobic sludge from an industrial digester that processes brewery wastewater under mesophilic conditions (35 °C), with the following characteristics: pH, 7.5±0.1; 54.9±0.6 g total solids (TS) L^{-1}, 47.2±0.4 g volatile solids (VS) L^{-1}; and total chemical oxygen demand (TCOD), 33.1±0.4 g O_2 L^{-1}. The initial inoculum concentration was set at 15 g VS L^{-1}, and the inoculum-to-substrate ratio (ISR) was set at 2 on a VS basis. A basal medium containing macro- and micro-nutrients, which was prepared and dosed as described elsewhere (Villamil et al., 2020b), was added and the vial was filled up to 60 mL with DW. The vials were closed with rubber stoppers and metallic crimps, flushed with N_2 for 2 min to ensure anaerobic conditions, and kept in a thermostatic water-bath at a mesophilic temperature of 35±1 °C and stirred at 100 rpm. The time-course of the AD experiment was recorded using 10 vials for each temperature studied. Seven vials were analysed: two during the first 3 days and then one per week. The remaining three vials were used to monitor the methane production. Blank samples were used in triplicate without any substrate to establish the background biogas level of the inoculum. In addition, starch-positive controls (Panreac, Darmstadt, Germany) were run in triplicate, yielding 341±10 mL STP CH_4 g^{-1} COD_{added}, to confirm the activity of the inoculum. The methane released was measured using volume displacement (removing CO_2 from the biogas by flushing through a 2 N NaOH solution) and expressed at standard temperature and pressure (STP: 273.14 K, 1 bar). The methane production of each reactor was monitored daily and calculated by subtracting the methane produced in the blank experiments. Liquid samples from the AD runs were filtered (0.45 μm) before analysis.

2.3. Characterisation of feedstock and hydrothermal carbonisation products

The elemental composition (C, H, N, and S) of the solid samples (feedstock and HC) was determined using a CHNS analyser (LECO CHNS-932; Geleen, The Netherlands). Proximate analysis (moisture, ash, VM, and fixed carbon (FC)) was performed using a Discovery SDT thermogravimetric analyser (TG 209, F3, Netzsch,; Selb, Germany)

according to the ASTM-D7582 standard (ASTM, 2015). The mineral elements were quantified using inductively coupled plasma atomic emission spectroscopy (ICP-OES) on an Elan 6000 Sciex instrument (Perkin Elmer). The HHV of the dried solid samples was estimated using Schuster's equation (Schuster et al., 2001; Eq. (1)):

$$HHV\left(MJ\ \ kg^{-1}\right) = 0.3491{\cdot}C(wt.\%) + 1.1783{\cdot}H(wt.\%) + 0.1005{\cdot}S(wt.\%) - 0.0151{\cdot}N(wt.\%) - 0.1034{\cdot}O(wt.\%) - 0.0211{\cdot}Ash(wt.\%) \quad (1)$$

The liquid samples (PW and centrifuged samples from the AD experiments) were characterised by measuring the pH (Crison 20 Basic pH-metre), TS, and VS according to standard methods 2540B and 2540E (APHA, 2005) and by measuring the TCOD (Raposo et al., 2008). The soluble COD (SCOD) was determined in accordance with the APHA method 5220D, and the total alkalinity (TA) was calculated by performing titration at a pH of 4.3 with 0.02 N H_2SO_4 (2320B). The total ammonia nitrogen (TAN) content was determined by distillation and titration (4500E) (APHA, 2005). The total organic carbon (TOC) content was determined using a Shimadzu TOC–VCPN analyser. The individual volatile fatty acid (VFA) (C2 to C7 including isoforms) values were determined via gas chromatography on a Varian 430-GC instrument equipped with a flame ionisation detector and a capillary column packed with nitroterephthalic acid-modified polyethylene glycol (Nukol) (De la Rubia et al., 2018a). The chemical species were identified using gas chromatography/ion-trap mass spectrometry on a CP-3800/Saturn 2200 instrument equipped with a Varian CP-8200 autosampler injector and a Carbowax/Divinyl benzene Yellow Green solid-phase micro-extractor, and fitted with a Factor Four VF-5 MS capillary column (De la Rubia et al., 2018a).

2.4. Prediction of ash fouling and slagging

The prediction of ash deposition during HC combustion plays an important role in decision making during real boiler operations. The propensity for fouling and slagging can be evaluated using the following equations:

$$R_{b/a} = \frac{(Fe_2O_3 + CaO + MgO + K_2O + NaO_2)(wt.\%)}{(SiO_2 + Al_2O_3 + TiO_2)(wt.\%)} \quad (2)$$

$$SI = R_{b/a}{\cdot}S_d \quad (3)$$

$$FI = R_{b/a}{\cdot}(K_2O + Na_2O)(wt.\%) \quad (4)$$

$$AI\left(kgGJ^{-1}\right) = \frac{1{\cdot}10^6{\cdot}(K_2O + Na_2O)(wt.\%)}{HHV(kJkg^{-1})} \quad (5)$$

where $R_{b/a}$ is the acid-base ratio, S_d is the sulphur content (wt.%), SI is the slagging index, FI is the fouling index, and AI is the alkaline index, which is defined as the amount of alkaline oxides in the HC per GJ (Cao et al., 2021).

2.5. Combustion and kinetic properties

Combustion experiments were performed under atmospheric pressure using a Discovery SDT 650 thermogravimetric analyser. The thermogravimetric analysis conditions are described elsewhere (Marin-Batista et al., 2020b). The Flynn-Wall-Ozawa (FWO) method is the most common approach used to describe combustion behaviour (Fan et al., 2017). It is based on first-order kinetics and uses Doyle's approach to evaluate the combustion behaviour of carbonaceous materials (Eq. (6)).

$$ln(\beta) = ln\left(\frac{A{\cdot}E_a}{R{\cdot}g(\alpha)}\right) - 5.331 - 1.052{\cdot}\frac{E_a}{R}{\cdot}\frac{1}{T} \quad (6)$$

where ln(β) is the linearisation of (E_a/R), A is the frequency or pre-exponential factor, E_a is the activation energy of the reaction (kJ mol^{-1}), R is the universal gas constant (kJ mol^{-1} K^{-1}), T is the absolute temperature (K), and g(α) is described using a first-order model: −ln(1 − α). E_a can be obtained from the slope of ln(β) vs. 1/T, whereas the pre-exponential factor (A) is calculated from the intercept of this straight line. The degree of conversion, α, is defined by Eq. (7).

$$\alpha = \frac{m_0 - m_f}{m_0 - m_\infty} \quad (7)$$

where m_0, m_∞, and m_f are the weights of the GPW and HC at the initial time t and final reaction stages, respectively.

Comprehensive combustion index (CCI) and thermodynamic parameters, including enthalpy (ΔH), Gibbs free energy (ΔG), and entropy (ΔS), were calculated using the following equations:

$$CCI\left(\min^{-2}\ \ C^{-3}\right) = \frac{(dw/dt)_{\max} - (dw/dt)_{mean}}{T_i^2{\cdot}T_b} \quad (8)$$

$$\Delta H(kJmol^{-1}) = Ea - R{\cdot}T \quad (9)$$

$$\Delta G\left(kJmol^{-1}\right) = Ea + \frac{R{\cdot}T_m{\cdot}ln(K_B \times T_m)}{h{\cdot}A} \quad (10)$$

$$\Delta S(Jmol^{-1}K^{-1}) = \frac{\Delta H - \Delta G}{T_m} \quad (11)$$

where $(dw/dt)_{max}$ indicates the maximum weight loss rate; $(dw/dt)_{mean}$ is the average weight loss rate; T_i, T_b, and T_m (°C) is the temperature of ignition, burn out, and the maximum weight loss, respectively; K_B is Boltzmann's constant (kg m^2 s^{-2} K^{-1}); and h is Planck's constant (kg m^2 s^{-1}).

Severity factor (SF) indicates the impact of temperature and reaction time on the HTC process and the products obtained. SF was defined based on the Arrhenius equation (Eq. (12)) (Chornet and Overend, 2017).

$$SF = log\left(t{\cdot}exp\left(\frac{T - 100}{14.75}\right)\right) \quad (12)$$

where t is the reaction time (min), T is the temperature (°C), and 14.75 is the activation energy based on the first-order cellulose degradation process (kJ mol^{-1}).

2.6. Energy balance

Equations (13)–(14) were used to calculate product mass yield. HC mass yield (Y_{HC}) is defined as the weight ratio of recovered HC (W_{HC}) to feedstock (W_{GPW}) on a dry basis. PW yield (Y_{PW}) is defined as the weight ratio of TS in the PW (TS) to the feedstock.

$$Y_{HC} = \frac{W_{HC}}{W_{GPW}} \quad (13)$$

$$Y_{PW} = \frac{TS}{W_{GPW}} \quad (14)$$

The specific methane production (SMP) (Nm^3 CH_4 kg^{-1} TCOD)

obtained from the batch anaerobic tests was converted into HHV_{PW} values using Eq. (15).

$$HHV_{PW}\left(MJ\ \ kg^{-1}\right) = 39.8 \cdot SMP \cdot \frac{TCOD}{TS} \quad (15)$$

where 39.8 is the lower heating value for pure methane (MJ Nm^{-3}), and the TCOD to TS ratio (kg TCOD kg^{-1} TS) is calculated from the PW.

The energy recovery associated with HTC products (HC and methane) was calculated using Eq. (16).

$$Energy\ \ recovered\ \ \left(MJ\ \ kg_{GPW}^{-1}\right) = HHV_{HC} \cdot Y_{HC} + HHV_{PW} \cdot Y_{PW} \quad (16)$$

The energy required for HTC was based on calculations of the energy required to heat the reactor, water, and biomass, according to Eq. (17) (Zhao et al., 2014):

$$E_{HTC,in} = \frac{\left(W_w \cdot \left(H_{l,HTC} - H_{l,amb}\right) + \left(W_{GPW} \cdot C_p + C_{bulk} + h_{bulk} \cdot A \cdot \tau\right) \cdot \left(T_{HTC} - T_{amb}\right)\right)}{\left(H_{g,HTC} - H_{l,HTC}\right)} \cdot \left(H_{g,HTC} - H_{l,amb}\right) \quad (17)$$

where W_w and W_{GPW} are the mass of water and solid in kg, respectively; $H_{l,HTC}$ and $H_{l,amb}$ are the enthalpies associated with carbonisation and that at room temperature in kJ kg^{-1}, respectively; T_{HTC} and T_{amb} are the temperatures associated with carbonisation and the ambient environment in K, respectively; C_{bulk} represents the energy required to heat the reactor vessel, which is calculated using the equation proposed by Namioka et al. (2008) and is equal to 1550 kJ K^{-1}; h_{bulk}·A is the convective heat transfer coefficient per unit surface area of the reactor and is equal to 115 kJ K^{-1}; C_p is the specific heat capacity of the sludge (1.7 kJ kg^{-1} K^{-1}); and τ is the holding time (h).

The HC was dewatered to exhibit a 40 wt.% moisture content by using a press filter, with an electricity consumption of 162 kJ kg^{-1} HC. Thereafter, the moisture of the HC was decreased to 8% via thermal drying, with an energy consumption of 2754 kJ kg^{-1} for evaporated water. The energy consumed to pump the PW to the anaerobic digester was 108 kJ kg^{-1} PW (Aragón-Briceño et al., 2020). The energy consumption of the pelletiser was 51 kJ kg^{-1} HC (Wang et al., 2020). Fig. 1 shows the process flowchart and energy inputs/outputs for each stage of integrated HTC and AD processes.

3. Results and discussion

3.1. Hydrochar characteristics

Table 1 presents the representative characterisation data (elemental analysis, fuel properties, energy assessment, proximal analysis, and prediction of slagging and fouling propensity) for GPW and HC. The carbon content and HHV of HC increased significantly with the carbonisation temperature, especially at 230 °C (10.2% in carbon content,

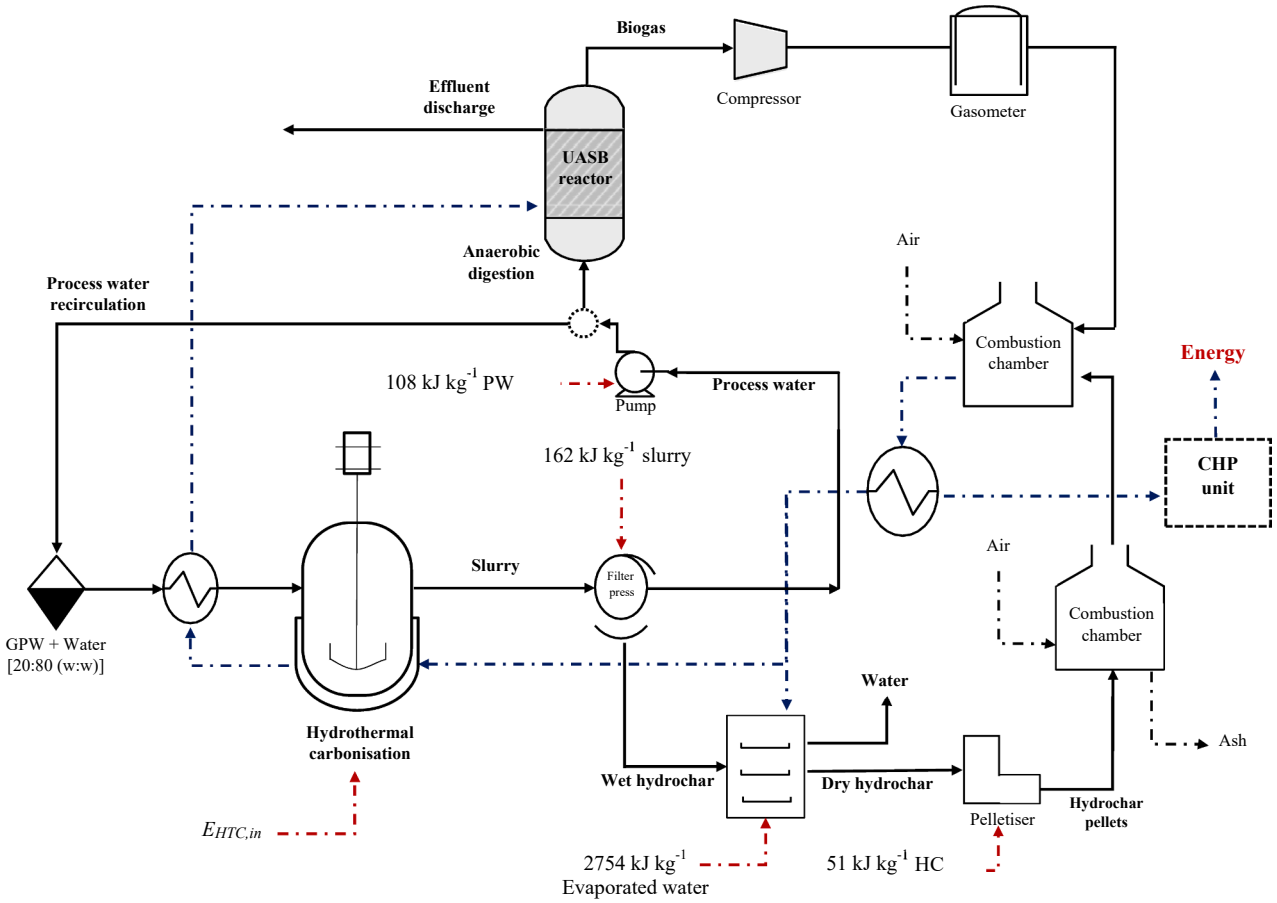

Fig. 1. Process flowchart and energy inputs/outputs for each stage of integrated HTC and AD processes. Red dashed lines represent energy inputs and blue dashed lines denote energy outputs.

Table 1
Main characteristics of garden and park wastes and hydrochars.

	GPW	HC180	HC210	HC230
C (%)	46.9 (1.1)	49.8 (0.2)	53.5 (0.1)	57.1 (0.1)
H (%)	6.1 (0.4)	5.3 (0.1)	5.4 (0.1)	5.3 (0.1)
N (%)	0.9 (0.1)	1.3 (0.1)	1.0 (0.1)	1.1 (0.1)
S (%)	0.4 (0.2)	0.2 (0.1)	0.1 (0.1)	0.1 (0.2)
O* (%)	40.6 (0.1)	40.1 (0.1)	36.3 (0.1)	31.4 (0.1)
H/C atomic ratio	1.55	1.29	1.21	1.11
O/C atomic ratio	0.65	0.60	0.51	0.41
Fuel ratio	0.24	0.44	0.42	0.56
Y_{HC} (%)	–	87.6 (0.2)	74.3 (0.2)	68.3 (0.2)
Severity factor	–	4.1	5.0	5.6
Energy densification	–	1.05	1.16	1.24
Energy yield (%)	–	18.1	16.6	16.7
HHV (MJ kg^{-1})	19.7 (0.1)	20.7 (0.1)	22.3 (0.1)	24.5 (0.1)
Volatile matter (%)	76.5 (0.1)	67.1 (0.1)	67.6 (0.1)	60.9 (0.1)
Fixed carbon (%)	18.4 (0.1)	29.6 (0.1)	28.6 (0.1)	34.1 (0.1)
Ash (%)	5.1 (0.1)	3.3 (0.1)	3.7 (0.1)	5.0 (0.1)
$R_{b/a}$	1.3	1.0	1.2	1.2
SI	0.53	0.16	0.15	0.16
FI	7.47	3.08	2.56	2.08
AI (kg GJ^{-1})	0.30	0.09	0.07	0.07

* Calculated from the mass balance: O = 100 − C − H − N − S − ash. Recommended limit values: AI < 0.17, safe combustion; 0.17 < AI < 0.34, probable slagging and fouling; AI > 0.34, almost certain slagging and fouling; Rb/a < 0.5, low slagging risk; SI < 0.6, low ash slagging inclination; 0.6 < SI < 2.0, medium ash slagging inclination; SI > 2.0, high ash slagging inclination FI < 0.6, low fouling; 0.6 < FI < 40.0 medium fouling; FI > 40.0 high fouling. Note: Standard deviation is indicated in parentheses.

and 24.3% for HHV, with respect to the raw material). HC mass yield in the HTC of lignocellulosic biomass is highly dependent on the composition of hemicellulose, cellulose, and lignin. Volpe et al. (2020) found that cellulose remained unaltered at temperatures up to 220 °C, and was almost completely decomposed at 230 °C; however, lignin was unchanged. Degradation of hemicellulose starts at temperatures above 180 °C. In this case, augmenting the carbonisation temperature above 220 °C increases the organic loading of the PW (De la Rubia et al., 2018a), which decreases the HC mass yield. This led to a decrease in Y_{HC} from 87.6% (180 °C) to 68.3% (230 °C) due to the transfer of low-molecular-weight compounds to the PW, which led to a significant decrease in the VM content (12–20%) with increasing temperature; this result implies that the components are easily hydrolysed. The lower CF and higher VM contents in HC210 are probably due to the formation of secondary HCs obtained through the polymerisation, recondensation, and aromatisation reactions of the hydrolysed molecules of the initial biomass (Ischia and Fiori, 2021; Lucian et al., 2019).

During the hydrolysis, dehydration, and decarboxylation reactions that are common in thermochemical processes, the biosolid loses H and O in the form of H_2O and CO_2, thereby increasing the partial carbon content in the solid. The O/C and H/C atomic ratios decreased with the carbonisation temperature, reaching the range of peat for HC180 and HC210 and that of lignite for HC230. Notably, fuels with low atomic O/C and H/C ratios are considered appropriate because they result in a low amount of smoke, water vapour, and energy loss during combustion (Liu et al., 2013). When the carbonisation temperature was increased, the fuel ratio (FC/VM) increased gradually from 0.24 for the feedstock to 0.54 for HC230, leading to an increase in the HHV as well as high stability and energy efficiency of HC during combustion. HC with similar characteristics (HHV: 20–29 MJ kg^{-1}, Y_{HC}: 50–70%, and %C: 49–72%) was obtained from other lignocellulosic biomass (corn stalk, olive trimmings, loblolly pine, and rice hulls) under similar operating conditions (Hoekman et al., 2017; Lucian et al., 2019; Lynam et al., 2015). The energy densification increased from 1.05 at 180 °C to 1.24 at 230 °C. However, the energy yield decreased correspondingly from 92% to 85%, owing to the HC yield. These ratios, which can be mathematically represented by the SF (Eq. (12)), reached values in the range of 4.1–5.6. Previous studies have shown that an SF above 4 is associated with a high level of charring, increased FC content, augmented energy densification, and enlarged HHV values, thereby exhibiting better characteristics for energy production (Gaur et al., 2020).

Similarly, the ash content decreased from 5.1% for GPW to 3.3% and 3.7% for HC180 and HC210, respectively, and reached values close to those of the raw material for HC230. HC showed a reduction in the amounts of K (50–72%), Na (27–39%), and Mg (16–26%) due to transfer of these elements to the PW (Table S1). Considering the values obtained for the slagging index (SI ≈0.2) and fouling index (FI ≈2.1–3.1), the combustion of HC obtained from GPW has a very low probability of forming slag (SI <0.6) and an intermediate probability of inducing fouling (FI <4) (Yang et al., 2019) because of the low Na and K contents in HC. The AI, which is the amount of slag generated per GJ of energy produced, decreased from 0.3 kg GJ^{-1} (GPW) to <0.1 kg GJ^{-1} (HC).

3.2. Combustion behaviour and kinetic parameters of hydrochar

Fig. 2 shows the thermogravimetric (TG) and differential thermogravimetric (DTG) data for the feedstock and HC. The TG and DTG curves of GPW and HC showed similar trends, with three different zones. In the preheating zone (30–250 °C), there was a slight weight loss of approximately 2–4%, corresponding to moisture evaporation. In the second or active zone, the samples rapidly lost up to 93 wt.%. In this zone, two different peaks were observed in the DTG curve. The first peak (250–400 °C) corresponds to the combustion of low-molecular-weight compounds (VM, hemicellulose, and cellulose), and the second peak (400–550 °C) is attributed to the degradation of high-molecular-weight compounds (lignin and FC) (Marin-Batista et al., 2020b). The areas under the first and second peaks decreased and increased with the carbonisation temperature, respectively, owing to the decomposition of low-molecular-weight compounds and insoluble organic compounds and their transfer to PW; however, lignin, which is very stable to hydrothermal processes, remained stable in the HC (Volpe et al., 2020). In the third zone, a small peak was observed for all samples (750–800 °C), which is mainly related to the decomposition of inorganic matter such as carbonates (Wang et al., 2019b).

Table S2 shows the main combustion characteristics of HC based on the TGA data. HC180 showed the highest CCI (8.0 × 10^{-7} min^{-2} °C^{-3}) and the lowest T_i (242 °C) and E_a (62.3 kJ mol^{-1}), indicating a higher combustion reactivity relative to HC210 and HC230. In addition, for HC180, the A value of >10^7 min^{-1} indicates high carbon coalition, higher calorific values, better combustion efficiency, and higher energy production rates (Barbanera et al., 2018; Yang et al., 2019). This was verified by thermodynamic analysis, where HC180 presented the lowest ΔH, ΔG, and ΔS values, which proves that less energy is required for the total combustion of this sample. Increasing the carbonisation severity (temperature) resulted in a slight decrease in the combustion reactivity of HC, mainly owing to the higher FC content. Thus, HC produced at high temperature requires longer retention times for complete combustion, which avoids the emission of polycyclic aromatic hydrocarbons and CO (Weiner et al., 2016). Moreover, Zhang et al. (2020) observed that the mixture of mineral coals, which showed low combustion reactivity, high activation energy, and resistance for complete combustion, could help decrease the activation energy and improve their combustion rate with HC mixture.

Finally, the characteristics of HC from GPW fulfilled the quality standards (HHV >18 MJ kg^{-1}, VM content <75%, sulphur content <0.2%, and nitrogen content < 2%) for T2 solid fuels produced from thermally treated biomass (ISO/TS 17225-8, 2016); thus, HC can be used as an industrial fuel without any restrictions. In this sense, the valorisation of GPW through HTC and the use of HC-like energy sources at the industrial level obeys the Directive (EU) 1999/31/EC and 2018/2001 (European Parliament, 2018), which stipulate that all 27 members of EU must eliminate waste disposal in landfills by 2030 and promote the use of renewable energies.

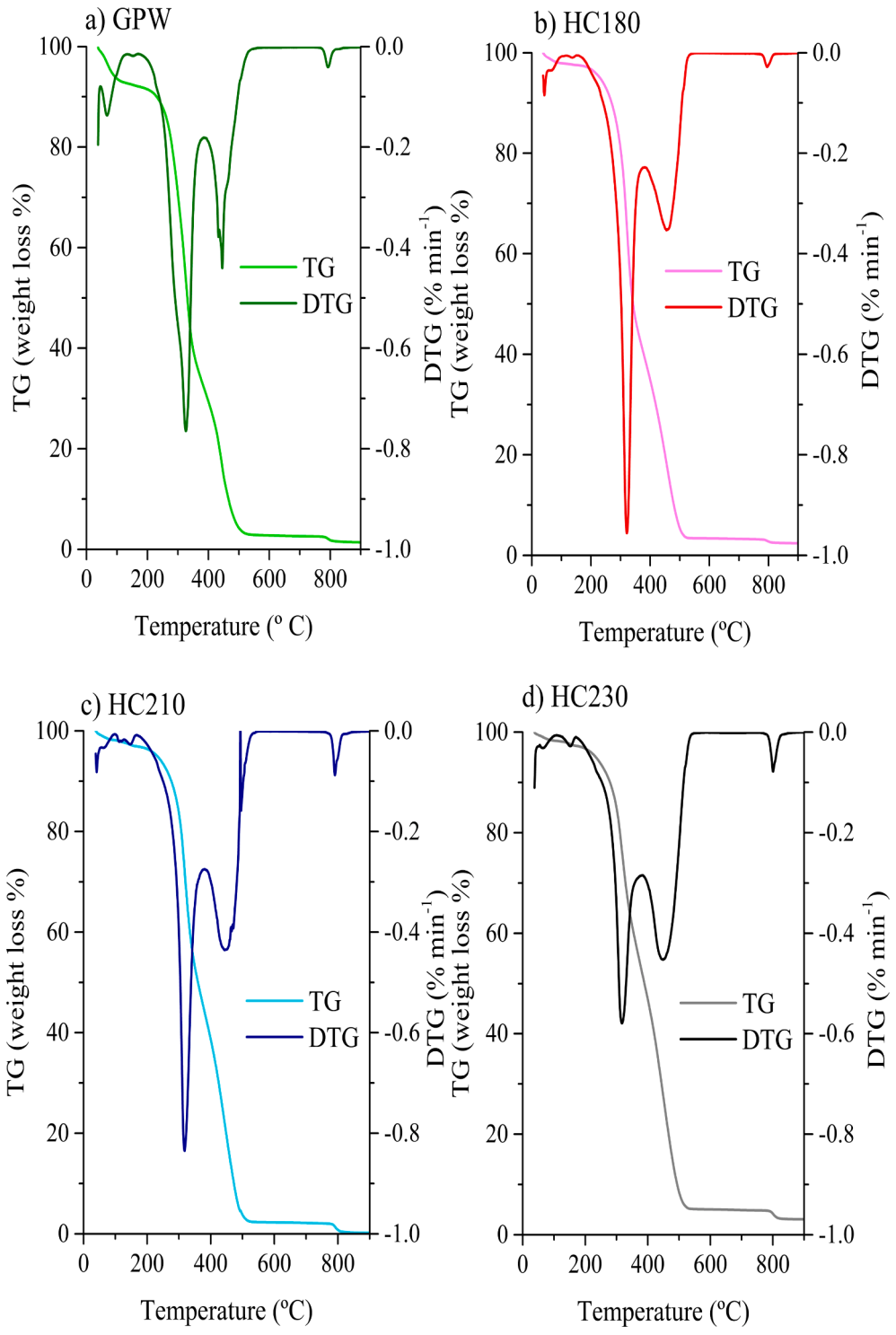

Fig. 2. Thermogravimetric and differential thermogravimetric profiles of raw feedstock and hydrochars.

Table 2
Main characteristics of process water.

	PW180	PW210	PW230
pH	3.5 (0.1)	3.4 (0.1)	3.5 (0.1)
TCOD (g L^{-1})	51.1 (1.3)	39.3 (0.5)	44.9 (2.4)
TOC (g L^{-1})	21.1 (0.1)	17.0 (0.1)	18.4 (0.1)
TS (g kg^{-1})	30.7 (0.3)	19.3 (0.3)	21.6 (0.4)
VS (g kg^{-1})	27.0 (0.4)	16.1 (0.2)	18.5 (0.3)

Note: Standard deviation is indicated in parentheses.

3.3. Anaerobic digestion of process water from hydrothermal carbonisation

Table 2 lists the main characteristics of the PW. The PW was acidic (pH ≈3.5) because of GPW hydrolysis, while exhibiting a high organic compound content, increased SCOD (39.3–51.1 g O_2 L^{-1}), and augmented TOC (17–21.1 g L^{-1}); therefore, treatment or valorisation is required prior to final disposal. An increase in HTC temperature from 180 to 210 °C favours the reactions of polymerisation, recondensation, and aromatisation associated with the formation of secondary HC,

thereby decreasing the content of TS (37%), SCOD (23%), and TOC (20%) in the PW. At 230 °C, cellulose hydrolysis (Volpe et al., 2020) induced an increase in these parameters. This is apparently related to the VM content of the HCs. In HC210, there was a slight increase in VM content (Table 1) at 210 °C, where there was a decrease in TS, SCOD, and TOC, relative to those in HC180 and HC230; this may indicate that these secondary HC have similar characteristics to those of VM, with a slightly lower molecular weight, but are thermally less stable than FC. Similar characteristics of the PW, such as acidic pH as well as high SCOD and TS values, were obtained via carbonisation of several lignocellulosic biomasses, such as pine sawdust, canola, vine, olive branches, and leaves (Pagés-Díaz et al., 2020).

Figs. S1 and S2 show the evolution of SCOD and the total volatile fatty acids (TVFA) during the AD process. The initial SCOD values were similar in all cases (~5 g O_2 L^{-1}). PW180 showed the greatest decline in the SCOD and TVFA of 65% and 72%, respectively. At the end of the runs, the SCOD reduction due to the TVFA was 23%. For PW210 and PW230, the TVFA declined minimally, and the SCOD remained unchanged (Fig. S2). This is probably because of the inhibition of methanogenic microorganisms due to the accumulation of propionic acid (>900 mg L^{-1}) (Villamil et al., 2020b) and/or the presence of inhibitory compounds, such as furfural, lignin monomers, and *N*- and *O*-heterocycles (Fig. S3 and Table S3). Therefore, it is assumed that the hydrolytic, acidogenic, and acetogenic stages developed normally during the AD of PW210 and PW230, but the methanogenic stage was severely affected.

In this way, as shown in Fig. 3, a higher methane yield was obtained for PW180 (326±3 mL CH_4 STP g^{-1} COD_{added}); however, for PW210 and PW230, the methane yield decreased by up to 24%, reaching values of 269±3 mL and 253±4 mL CH_4 STP g^{-1} COD_{added}, respectively. An increase in temperature in the HTC negatively affects the biodegradability of the liquid fraction because of the release of high-molecular-weight and aromatic compounds into this phase, which are poorly biodegradable under anaerobic conditions (De la Rubia et al., 2018a; Gaur et al., 2020). The methane yields from AD of the PW were higher than those obtained for GPW (75±3 mL CH_4 STP g^{-1} COD_{added}) without pretreatment. These results are similar to those reported for AD of the PW from orange pomace (195–253 CH_4 STP g^{-1} COD_{added}), microalgae (188–356 mL CH_4 STP g^{-1} COD_{added}), and pine sawdust (253 CH_4 STP g^{-1} COD_{added}) (Erdogan et al., 2015; Marin-Batista et al., 2019; Pagés-Díaz et al., 2020), which were obtained under conditions similar to those in the present study. The parameters, such as pH (7.5–7.8), TA (>2.5 g $CaCO_3$ L^{-1}) and TAN (<1700 mg N-NH_3 L^{-1}), were adequate for the AD process (De la Rubia et al., 2018b) in all tests.

The experimental results were fitted with a first-order model (PW180) and a modified Gompertz model (PW210 and PW230). Table 3

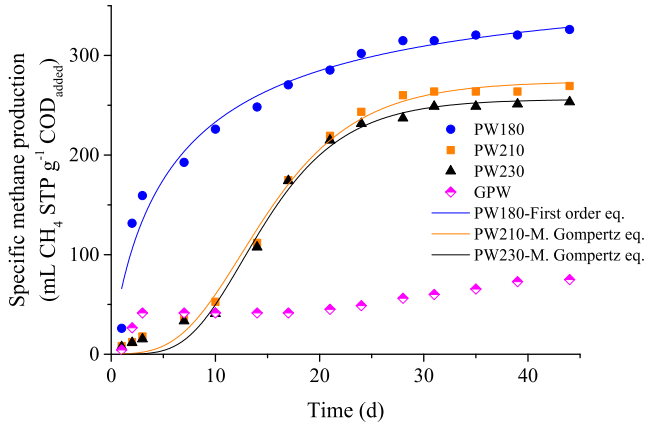

Fig. 3. Cumulative methane yield. Symbols represent experimental values, and solid lines indicate theoretical values (first-order for PW180 and modified Gompertz model for PW210 and PW230).

Table 3
Experimental maximum methane yield and fitting parameters.

Experimental	PW180	PW210	PW230
G_{me} (STP mL CH_4 g^{-1} COD_{added})	326 (3)	269 (3)	253 (4)
Model	**First-order**	**Modified Gompertz**	
G_{max} (STP mL CH_4 g^{-1} COD_{added})	325 ± 11	274 ± 6	256 ± 5
μ (mL CH_4 g^{-1} COD_{added} d^{-1})	–	16.78 ± 1.36	17.83 ± 1.63
k (d^{-1})	0.16 ± 0.02	–	–
λ (d)	–	6.5 ± 0.7	7.3 ± 0.7
R^2	0.912	0.992	0.992

Note: Standard errors are indicated by ± and standard deviation is presented in parentheses.

shows the fit between experimental and theoretical methane yields. PW180 methane production occurred without the presence of a latency period and presented a k value of 0.159 d^{-1}, which is in the same range as that previously reported by Ferreira et al. (2013) for steam explosion-pre-treated wheat straw AD at 150–220 °C (0.085–0.175 d^{-1}), but with a lower methane yield (159–273 mL CH_4 g^{-1} VS). This k value (0.159 d^{-1}) is below the commonly considered ideal value for rapid methane production (0.2–0.7 d^{-1}) (Nyktari et al., 2017). The modified Gompertz model also showed a good fit for the methane production of PW210 and PW230, given a lag phase of approximately 7 d, probably owing to the acclimation of the inoculum to the substrate. Similar behaviour was observed by De la Rubia et al. (2018b), where an acclimation period of 5–7 d was required for the AD of sewage sludge PW.

High HTC temperatures were associated with a decrease in the peak area of the alkyl and non-aromatic compounds (alcohols, cyclic chains, acids, and nitrogenous compounds; Fig. S3 and Table S3). Correspondingly, a wide variety of lignin monomers (aromatic and phenol compounds) and *N*- and *O*-heterocyclic compounds (pyrazines, pyrimidines, and pyridines) obtained from the degradation of sugars and reactions such as polymerisation, condensation, aromatisation, and Maillard reactions were detected (Fig. S3 and Table S3). After AD, the peak area of short chain alkyl compounds was reduced in all runs (Fig. S3). However, this reduction was not observed for the long-chain alkyl compounds (2-hexene, 2-ethyl-1-hexanol, 2-ethoxy propane, 1-tetradecanol) and N- and O-heterocyclic compounds (3-methyl-1H-indole, 1,3-dioxolane, phenol, 3-methyl-benzenamine), owing to the high stability of these molecules to the shielding effect and the lower loading density, respectively. In addition, as short-chain compounds, benzaldehyde, furans, and amines were also removed during AD because of the high reactivity of the carbonyl group (C=O) and O–H bond (Liu et al., 2019), thereby facilitating their oxidation by the action of anaerobic microorganisms. This is consistent with the study of Marin-Batista et al. (2019), who reported that AD completely removed the aldehydes and esters and partially removed the aromatic hydrocarbons from the PW obtained from HTC of microalgae. The removal of these compounds was more significant for PW180. The detection of methyl-1H-indole in PW210 and PW230, which can be degraded by methanogenic microorganisms (Marin-Batista et al., 2019), at the end of AD suggests the inhibition of the methanogenic process; this result is related to the high propionic acid concentration and low biodegradability of *N*- and *O*-compounds, which may result in poor stability of the AD process.

3.4. Energy evaluation of the synergistic HTC-AD process

Fig. 4 shows the maximum energy recovery from the AD of GPW and its treatment using the coupled HTC-AD process. The HHV of the GPW dry feedstock (19.7 MJ kg^{-1}) was considered as the total amount of energy stored in the feedstock (see Table 1). The percentage energy recovery for the AD of GPW was only 14% of the energy stored in the feedstock (2.8 MJ kg^{-1}), which is associated with the low degradability of GPW mentioned above. The percentage energy recovery is the same as that obtained for AD of the PW obtained at the three HTC temperatures

Table 4
Energy assessment of hydrothermal carbonisation and anaerobic digestion.

	Energy input (kWh t^{-1} feedstock)						Energy output (kWh t^{-1} feedstock)			Net energy (kWh t^{-1} feedstock)
	HTC reactor	Dewatering	Thermal dry	Pelletiser	Pump	Total input	Energy HC	Energy CH_4	Total output	
HTC180	364	8	82	9	7	469	1008	79	1086	617
HTC210	505	9	65	7	13	599	921	128	1048	449
HTC230	462	9	63	7	14	555	930	152	1082	527

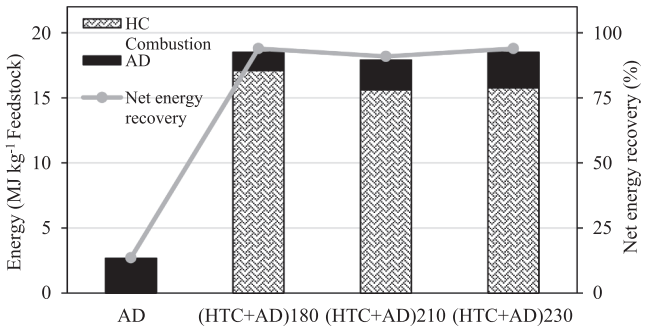

Fig. 4. Total energy recovery and net energy recovery for the valorisation of GPW through AD only and through HTC and AD processes.

(1.4–2.7 MJ kg^{-1}dry feedstock). Nevertheless, the synergy between HTC and AD produced a higher energy recovery owing to the HHV and yield of HC. The combustion of HC provided an energy of 16.7–18.3 MJ kg^{-1} dry feedstock, which when combined with the energy sourced from the methane combustion performed using PW, gave rise to a total energy recovery of 91–94% relative to that of the raw material. The high Y_{HC} value of HC180 and the high organic removal efficiency during the AD of PW180 indicate that the HTC process at the lowest working temperature (180 °C) is the best option for the valorisation of GPW, owing to the physicochemical characteristics of HC, its high energy recovery, and the high biodegradability of PW that led to the highest methane yield. Moreover, the integration of HTC and AD is the most cost-effective option when compared to using conventional AD, as determined by Villamil et al. (2019) for sewage sludge, which produces 4.4 times more energy than conventional AD of mixed sludge. In this case, combining the HTC and AD resulted in 6–6.5 times higher energy than that produced via direct AD of the GPW. The effluent from AD can be recirculated and combined with the GPW to obtain the necessary mixture to achieve an environmentally friendly process and avoid excessive water consumption in the HTC process.

Fig. 1 shows a flow chart of the combined process (HTC and AD). The GPW, which is mixed with water in a 20:80 wt.% (biomass/water) ratio, is preheated in a heat exchanger using waste energy from the HTC reactor. The obtained slurry is separated by a filter press, and the HC is dried and pelletised to be used as solid fuel. A part of the PW is recirculated to the carbonisation reactor, whereas the rest is sent to AD for biogas production. The AD process is performed in an upflow anaerobic sludge blanket (UASB) reactor, which allows the treatment of liquid waste with high organic load and minimal sludge formation. The effluent from the AD will be sent to an urban sewer system to complete the water treatment according to Directive 91/271/EEC (Pistocchi et al., 2019). The energy obtained from the combustion of HC and biogas will be used to carry out the HTC process, and the surplus thermal energy will be transformed into electrical energy through cogeneration units (Combined Heat and Power) (Heidari et al., 2020). Recirculation of the liquid fraction of the HTC can reduce water consumption in the GPW: water mixture, thus improving the properties of the resulting HC through the formation of secondary HC as well (Lucian et al., 2019; Picone et al., 2021).

Table 4 provides information (energy input and output) for establishing the energy balance for the HTC and AD coupled process at 180 °C, where these operating conditions afford the highest net energy production based on the high Y_{HC} and HHV values and methane yield. The energy from HC combustion (930–1008 kWh t^{-1} feedstock) was high enough to meet the energy demands (499–599 kWh t^{-1} feedstock) of all the stages involved ($E_{HTC,in}$, dewatering, thermal drying, pelletising, and pumping), resulting in a completely autothermal process. The energy surplus from the combustion of HC and biogas was up to 2.4 times greater than the energy needed to carry out the entire HTC process. Moreover, with the addition of a heat recovery stage by placing a heat exchanger before the HTC reactor inlet, the overall efficiency of the process could be significantly increased, thereby reducing the energy demand by up to 50% (Mendecka et al., 2020). According to Ingelia (2021), surplus energy could be sold at a market price of 32 MWh^{-1}. Considering the surplus energy and following the approach taken by Heidari et al. (2020), where the thermal energy surplus is transformed into electrical energy with an efficiency of 33% through the use of high- and low-pressure turbines, the economic benefits from energy sale could range from 115 to 160 € d^{-1}. Therefore, the combination of thermochemical and biological processes (HTC and AD) allows for obtaining high energy recovery with minimal generation of pollutant streams.

4. Conclusions

HTC is a promising and viable process for valorising and improving the physicochemical properties of GPW and maximising the energy density, with increased energy savings and very high cost-effectiveness. The HC obtained in the studied temperature range (180–230 °C) presents physicochemical characteristics suitable for industrial use as a solid fuel (high HHV as well as low ash, nitrogen, and sulphur contents), fulfilling the requirements of the ISO 17225-8 standard. Furthermore, HC obtained at 180 °C presents the optimal characteristics for combustion (low ignition temperature, energy activation, comprehensive combustibility index, and high mass-loss rate), which are attributed to its physicochemical characteristics. Likewise, AD of the PW produced via the HTC of GPW is an interesting alternative for enhancing the overall process, thereby improving the energy recovery, reducing the load of organic compounds, closing the valorisation cycle of biomass and generating a circular economy, and allowing the integration of HTC and AD with promising results. The AD of PW obtained at 180 °C presents the highest methane yield (326 mL CH_4 STP g^{-1} COD_{added}) and organic matter removal (≈ 65%). Coupling thermochemical and biological processes (HTC and AD) may be favourable for renewable energy production and can promote the development of a circular economy, where up to 94% of the energy of raw biomass (GPW) is recovered with a positive energy balance. In this respect, only a part of the energy from HC combustion (43–51%) is required to make the HTC process self-sufficient, and the remaining energy can be used for electricity production via the Brayton cycle.

CRediT authorship contribution statement

R.P. Ipiales: Investigation, Writing – original draft. **A.F. Mohedano:** Conceptualization, Funding acquisition, Methodology, Resources, Writing – review & editing, Supervision, Project administration. **E. Diaz:** Validation, Funding acquisition, Methodology, Resources, Writing –

review & editing. **M.A. de la Rubia:** Conceptualization, Validation, Funding acquisition, Methodology, Supervision, Writing – review & editing, Supervision.

Declaration of Competing Interest

The authors declare that they have no known competing financial interests or personal relationships that could have appeared to influence the work reported in this paper.

Acknowledgements

The authors gratefully acknowledge funding from Spain's MINECO (PID2019-108445RB-I00; PDC2021-120755-I00) and the Comunidad de Madrid (Project S2018/EMT-4344). R. P. Ipiales acknowledges financial support from the Comunidad de Madrid (IND2019/AMB-17092) and the Arquimea-Agrotech Company.

Appendix A. Supplementary material

Supplementary data to this article can be found online at https://doi.org/10.1016/j.wasman.2022.01.003.

References

Ahmed, M., Andreottola, G., Elagroudy, S., Negm, M.S., Fiori, L., 2021. Coupling hydrothermal carbonization and anaerobic digestion for sewage digestate management: Influence of hydrothermal treatment time on dewaterability and bio-methane production. J. Environ. Manage. 281, 111910. https://doi.org/10.1016/j.jenvman.2020.111910.

Antero, R.V.P., Alves, A.C.F., de Oliveira, S.B., Ojala, S.A., Brum, S.S., 2020. Challenges and alternatives for the adequacy of hydrothermal carbonization of lignocellulosic biomass in cleaner production systems: A review. J. Clean. Prod. 252, 119899. https://doi.org/10.1016/j.jclepro.2019.119899.

APHA, 2005. Standard methods for the examination of water and wastewater. American Public Health Association, 21st ed. Washington, DC., USA.

Aragón-Briceño, C.I., Grasham, O., Ross, A.B., Dupont, V., Camargo-Valero, M.A., 2020. Hydrothermal carbonization of sewage digestate at wastewater treatment works: Influence of solid loading on characteristics of hydrochar, process water and plant energetics. Renew. Energy 157, 959–973. https://doi.org/10.1016/j.renene.2020.05.021.

Aragón-Briceño, C.I., Pozarlik, A.K., Bramer, E.A., Niedzwiecki, L., Pawlak-Kruczek, H., Brem, G., 2021. Hydrothermal carbonization of wet biomass from nitrogen and phosphorus approach: A review. Renew. Energy 171, 401–415. https://doi.org/10.1016/j.renene.2021.02.109.

Araújo, Y.R.V., de Góis, M.L., Junior, L.M.C., Carvalho, M., 2018. Carbon footprint associated with four disposal scenarios for urban pruning waste. Environ. Sci. Pollut. Res. 25 (2), 1863–1868. https://doi.org/10.1007/s11356-017-0613-y.

ASTM, 2015. Standard test methods for proximate analysis of coal and coke by macro thermogravimetric analysis. Method D7582-15. ASTM-International, Pennsylvania.

Barbanera, M., Cotana, F., Di Matteo, U., 2018. Co-combustion performance and kinetic study of solid digestate with gasification biochar. Renew. Sustain. Energy Rev. 121, 597–605. https://doi.org/10.1016/j.renene.2018.01.076.

Bardhan, M., Novera, T.M., Tabassum, M., Islam, M.A., Islam, M.A., Hameed, B.H., 2021. Co-hydrothermal carbonization of different feedstocks to hydrochar as potential energy for the future world: A review. J. Clean. Prod. 298, 126734. https://doi.org/10.1016/j.jclepro.2021.126734.

Bargmann, I., Rillig, M.C., Kruse, A., Greef, J.-M., Kücke, M., 2014. Effects of hydrochar application on the dynamics of soluble nitrogen in soils and on plant availability. J. Plant Nutr. Soil Sci. 177 (1), 48–58. https://doi.org/10.1002/jpln.201300069.

Cao, Z., Hülsemann, B., Wüst, D., Oechsner, H., Lautenbach, A., Kruse, A., 2021. Effect of residence time during hydrothermal carbonization of biogas digestate on the combustion characteristics of hydrochar and the biogas production of process water. Bioresour. Technol. 333, 125110. https://doi.org/10.1016/j.biortech.2021.125110.

Chornet, E., Overend, R.P., 2017. How the severity factor in biomass hydrolysis came about, Hydrothermal Processing in Biorefineries: Production of Bioethanol and High Added-Value Compounds of Second and Third Generation. In: Ruiz, H.A., Hedegaard Thomsen, M., Trajano, H.L. (Eds.), Hydrothermal Processing in Biorefineries. Springer International Publishing, Cham, pp. 1–3. https://doi.org/10.1007/978-3-319-56457-9_1.

De la Rubia, M.A., Villamil, J.A., Rodriguez, J.J., Borja, R., Mohedano, A.F., 2018a. Mesophilic anaerobic co-digestion of the organic fraction of municipal solid waste with the liquid fraction from hydrothermal carbonization of sewage sludge. Waste Manag. 76, 315–322. https://doi.org/10.1016/j.wasman.2018.02.046.

De la Rubia, M.A., Villamil, J.A., Rodriguez, J.J., Mohedano, A.F., 2018b. Effect of inoculum source and initial concentration on the anaerobic digestion of the liquid fraction from hydrothermal carbonisation of sewage sludge. Renew. Energy 127, 697–704. https://doi.org/10.1016/j.renene.2018.05.002.

Diaz, E., Manzano, F.J., Villamil, J., Rodriguez, J.J., Mohedano, A.F., 2019. Low-cost activated grape seed-derived hydrochar through hydrothermal carbonization and chemical activation for sulfamethoxazole adsorption. Appl. Sci. 9 (5127), 1–14. https://doi.org/10.3390/app9235127.

Erdogan, E., Atila, B., Mumme, J., Reza, M.T., Toptas, A., Elibol, M., Yanik, J., 2015. Characterization of products from hydrothermal carbonization of orange pomace including anaerobic digestibility of process liquor. Bioresour. Technol. 196, 35–42. https://doi.org/10.1016/j.biortech.2015.06.115.

European Parliament, 2018. Directive (EU) 2018/2001 of the European Parliament and of the Council on the promotion of the use of energy from renewable sources, Official Journal of the European Union.

EUROSTAT, 2019. Energy, transport and environment statistics. Belgium. https://doi.org/10.2785/499987.

Fan, F., Zheng, Y., Huang, Y., Lu, Y., Wang, Z., Chen, B., 2017. Combustion kinetics of biochar prepared by pyrolysis of Macadamia shells. Bioresour. Technol. 12, 3918–3932. https://doi.org/10.15376/biores.12.2.3918-3932.

Fang, J., Zhan, L., Sik, Y.O., Gao, B., 2018. Minireview of potential applications of hydrochar derived from hydrothermal carbonization of biomass. J. Ind. Eng. Chem. 57, 15–21. https://doi.org/10.1016/j.jiec.2017.08.026.

Ferreira, L.C., Donoso-Bravo, A., Nilsen, P.J., Fdz-Polanco, F., Pérez-Elvira, S.I., 2013. Influence of thermal pretreatment on the biochemical methane potential of wheat straw. Bioresour. Technol. 143, 251–257. https://doi.org/10.1016/j.biortech.2013.05.065.

Gaur, R.Z., Khoury, O., Zohar, M., Poverenov, E., Darzi, R., Laor, Y., Posmanik, R., 2020. Hydrothermal carbonization of sewage sludge coupled with anaerobic digestion: Integrated approach for sludge management and energy recycling. Energy Convers. Manag. 224, 113353. https://doi.org/10.1016/j.enconman.2020.113353.

Heidari, M., Salaudeen, S., Norouzi, O., Acharya, B., Dutta, A., 2020. Numerical comparison of a combined hydrothermal carbonization and anaerobic digestion system with direct combustion of biomass for power production. Processes 8 (43), 1–13. https://doi.org/10.3390/pr8010043.

Hoekman, S.K., Broch, A., Felix, L., Farthing, W., 2017. Hydrothermal carbonization (HTC) of loblolly pine using a continuous, reactive twin-screw extruder. Energy Convers. Manag. 134, 247–259. https://doi.org/10.1016/j.enconman.2016.12.035.

Ingelia, 2021. Ingelia [WWW Document]. URL https://ingelia.com/.

Ipiales, R.P., de la Rubia, M.A., Diaz, E., Mohedano, A.F., Rodriguez, J.J., 2021. Integration of Hydrothermal Carbonization and Anaerobic Digestion for Energy Recovery of Biomass Waste: An Overview. Energy Fuels 35 (21), 17032–17050.

Ischia, G., Fiori, L., 2021. Hydrothermal carbonization of organic waste and biomass: A review on process, reactor and plant modeling. Waste Biomass Valorization 12 (6), 2797–2824. https://doi.org/10.1007/s12649-020-01255-3.

Islam, Md Azharul, Limon, M.S.H., Romić, M., Atikul, I.M., 2021. Hydrochar-based soil amendments for agriculture: A review of recent progress. Arab. J. Geosci. 14 (102), 1–16. https://doi.org/10.1007/s12517-020-06358-8.

ISO/TS 17225-8, 2016. International organization for standardization ISO/TS 17225-8. Solid biofuels — Fuel specifications and classes. Graded thermally treated and densified biomass fuels. First edition. USA.

Kambo, H.S., Dutta, A., 2015. A comparative review of biochar and hydrochar in terms of production, physico-chemical properties and applications. Renew. Sustain. Energy Rev. 45, 359–378. https://doi.org/10.1016/j.rser.2015.01.050.

Langone, M., Sabia, G., Petta, L., Zanetti, L., Leoni, P., Basso, D., 2021. Evaluation of the aerobic biodegradability of process water produced by hydrothermal carbonization and inhibition effects on the heterotrophic biomass of an activated sludge system. J. Environ. Manage. 299, 113561. https://doi.org/10.1016/j.jenvman.2021.113561.

Lentz, Z., Kolar, P., Classen, J.J., 2019. Valorization of swine manure into hydrochars. Processes 7, 1–12. https://doi.org/10.3390/pr7090560.

Liu, R., Hao, X., van Loosdrecht, M.C.M., Zhou, P., Li, J.i., 2019. Dynamics of humic substance composition during anaerobic digestion of excess activated sludge. Int. Biodeterior. Biodegrad. 145, 104771. https://doi.org/10.1016/j.ibiod.2019.104771.

Liu, Z., Quek, A., Hoekman, S.K., Balasubramanian, R., 2013. Production of solid biochar fuel from waste biomass by hydrothermal carbonization. Fuel 103, 943–949. https://doi.org/10.1016/j.fuel.2012.07.069.

Lucian, M., Volpe, M., Fiori, L., 2019. Hydrothermal carbonization kinetics of lignocellulosic agro-wastes: Experimental data and modeling. Energies 12, 1–20. https://doi.org/10.3390/en12030516.

Lucian, M., Volpe, M., Merzari, F., Wüst, D., Kruse, A., Andreottola, G., Fiori, L., 2020. Hydrothermal carbonization coupled with anaerobic digestion for the valorization of the organic fraction of municipal solid waste. Bioresour. Technol. 314, 123734. https://doi.org/10.1016/j.biortech.2020.123734.

Lynam, J.G., Reza, M.T., Yan, W., Vásquez, V.R., Coronella, C.J., 2015. Hydrothermal carbonization of various lignocellulosic biomass. Biomass Conv. Bioref. 5 (2), 173–181. https://doi.org/10.1007/s13399-014-0137-3.

Marin-Batista, J.D., Mohedano, A.F., Rodríguez, J.J., De la Rubia, M.A., 2020a. Energy and phosphorous recovery through hydrothermal carbonization of digested sewage sludge. Waste Manag. 105, 566–574. https://doi.org/10.1016/j.wasman.2020.03.004.

Marin-Batista, J.D., Villamil, J.A., Qaramaleki, S.V., Coronella, C.J., Mohedano, A.F., De la Rubia, M.A., 2020b. Energy valorization of cow manure by hydrothermal carbonization and anaerobic digestion. Renew. Energy 160, 623–632. https://doi.org/10.1016/j.renene.2020.07.003.

Marin-Batista, J.D., Villamil, J.A., Rodriguez, J.J., Mohedano, A.F., De la Rubia, M.A., 2019. Valorization of microalgal biomass by hydrothermal carbonization and anaerobic digestion. Bioresour. Technol. 274, 395–402. https://doi.org/10.1016/j.biortech.2018.11.103.

Medina-Martos, E., Istrate, I.-R., Villamil, J.A., Gálvez-Martos, J.-L., Dufour, J., Mohedano, Á.F., 2020. Techno-economic and life cycle assessment of an integrated

hydrothermal carbonization system for sewage sludge. J. Clean. Prod. 277, 122930. https://doi.org/10.1016/j.jclepro.2020.122930.
Mendecka, B., Lombardi, L., Micali, F., De Risi, A., 2020. Energy Recovery from Olive Pomace by Hydrothermal Carbonization on Hypothetical Industrial Scale: A LCA Perspective. Waste Biomass Valorizat. 11 (10), 5503–5519. https://doi.org/10.1007/s12649-020-01212-0.
Namioka, T., Miyazaki, M., Morohashi, Y., Umeki, K., Yoshikawa, K., 2008. Modeling and analysis of batch-type thermal sludge pretreatment for optimal design. J. Environ. Eng. 3 (1), 170–181. https://doi.org/10.1299/jee.3.170.
Nyktari, E., Danso-Boateng, E., Wheatley, A., Holdich, R., 2017. Anaerobic digestion of liquid products following hydrothermal carbonisation of faecal sludge at different reaction conditions. Desalin. Water Treat. 91, 245–251. https://doi.org/10.5004/dwt.2017.20782.
Pagés-Díaz, J., Cerda, A., Montalvo, S., Diaz-Robles, L., Curio, C.H., 2020. Anaerobic biomethane potential of the liquors from hydrothermal carbonization of different lignocellulose biomasses. Renew. Energy 157, 182–189. https://doi.org/10.1016/j.renene.2020.05.025.
Picone, A., Volpe, M., Messineo, A., 2021. Process Water Recirculation during Hydrothermal Carbonization of Waste Biomass: Current Knowledge and Challenges. Energies 14, 2962. https://doi.org/10.3390/en14102962.
Pistocchi, A., Dorati, C., Grizzetti, B., Udias, A., Vigiak, O., Zanni, M., 2019. Water quality in Europe: Effects of the Urban Wastewater Treatment Directive. https://doi.org/10.2760/303163.
Raposo, F., Delarubia, M., Borja, R., Alaiz, M., 2008. Assessment of a modified and optimised method for determining chemical oxygen demand of solid substrates and solutions with high suspended solid content. Talanta 76 (2), 448–453. https://doi.org/10.1016/j.talanta.2008.03.030.
Reza, M.T., Freitas, A., Yang, X., Coronella, C.J., 2016. Wet Air Oxidation of Hydrothermal Carbonization (HTC) Process Liquid. ACS Sustain. Chem. Eng. 4 (6), 3250–3254. https://doi.org/10.1021/acssuschemeng.6b00292.
Reza, M.T., Lynam, J.G., Uddin, M.H., Coronella, C.J., 2013. Hydrothermal carbonization: Fate of inorganics. Biomass Bioenerg. 49, 86–94. https://doi.org/10.1016/j.biombioe.2012.12.004.
Schonvogel, D., Nowotny, M., Woriescheck, T., Multhaupt, H., Wagner, P., Dyck, A., Agert, C., Wark, M., 2019. Hydrothermal carbonization-derived carbon from waste biomass as renewable Pt support for fuel cell applications: Role of carbon activation. Energy Technol. 7 (11), 1900344. https://doi.org/10.1002/ente.v7.1110.1002/ente.201900344.
Schuster, G., Weigl, K., Hofbauer, H., 2001. Biomass steam gasification and extensive parametric modeling study. Bioresour. Technol. 77, 71–79. https://doi.org/10.1016/S0960-8524(00)00115-2.
Villamil, J.A., De la Rubia, M.A., Diaz, E., Mohedano, A.F., 2019. Technologies for wastewater sludge utilization and energy production: Hydrothermal carbonization of lignocellulosic biomass and sewage sludge. Wastewater Treatment Residues as Resources for Biorefinery Products and Biofuels 133–153. https://doi.org/10.1016/B978-0-12-816204-0.00007-2.
Villamil, J.A., Diaz, E., De la Rubia, M.A., Mohedano, A.F., 2020a. Potential use of waste activated sludge hydrothermally treated as a renewable fuel or activated carbon precursor. Molecules 25 (3524), 1–16. https://doi.org/10.3390/molecules25153534.
Villamil, J.A., Mohedano, A.F., San Martín, J., Rodriguez, J.J., De la Rubia, M.A., 2020b. Anaerobic co-digestion of the process water from waste activated sludge hydrothermally treated with primary sewage sludge. A new approach for sewage sludge management. Renew. Energy 146, 435–443. https://doi.org/10.1016/j.renene.2019.06.138.
Volpe, M., Messineo, A., Mäkelä, M., Barr, M.R., Volpe, R., Corrado, C., Fiori, L., 2020. Reactivity of cellulose during hydrothermal carbonization of lignocellulosic biomass. Fuel Process. Technol. 206, 106456. https://doi.org/10.1016/j.fuproc.2020.106456.
Wang, L., Chang, Y., Liu, Q., 2019a. Fate and distribution of nutrients and heavy metals during hydrothermal carbonization of sewage sludge with implication to land application. J. Clean. Prod. 225, 972–983. https://doi.org/10.1016/j.jclepro.2019.03.347.
Wang, R., Lin, K., Ren, D., Peng, P., Zhao, Z., Yin, Q., Gao, P., 2022. Energy conversion performance in co-hydrothermal carbonization of sewage sludge and pinewood sawdust coupling with anaerobic digestion of the produced wastewater. Sci. Total Environ. 803, 149964. https://doi.org/10.1016/j.scitotenv.2021.149964.
Wang, T., Li, Y., Zhi, D., Lin, Y., He, K., Liu, B., Mao, H., 2019b. Assessment of combustion and emission behavior of corn straw biochar briquette fuels under different temperatures. J. Environ. Manage. 250, 109399. https://doi.org/10.1016/j.jenvman.2019.109399.
Wang, Y., Qiu, L., Zhu, M., Sun, G., Zhang, T., Kang, K., 2019c. Comparative evaluation of hydrothermal carbonization and low temperature pyrolysis of Eucommia ulmoides oliver for the production of solid biofuel. Sci. Rep. 9, 1–11. https://doi.org/10.1038/s41598-019-38849-4.
Wang, Z., Zhai, Y., Wang, T., Wang, B., Peng, C., Li, C., 2020. Pelletizing of hydrochar biofuels with organic binders. Fuel 280, 118659. https://doi.org/10.1016/j.fuel.2020.118659.
Weide, T., Brügging, E., Wetter, C., 2019. Anaerobic and aerobic degradation of wastewater from hydrothermal carbonization (HTC) in a continuous, three-stage and semi-industrial system. J. Environ. Chem. Eng. 7 (1), 102912. https://doi.org/10.1016/j.jece:2019.102912.
Weiner, B., Wedwitschka, H., Poerschmann, J., Kopinke, F.-D., 2016. Utilization of Organosolv Waste Waters as Liquid Phase for Hydrothermal Carbonization of Chaff. ACS Sustain. Chem. Eng. 4 (10), 5737–5742. https://doi.org/10.1021/acssuschemeng.6b01665.
Yang, G., Yang, Z., Zhang, J., Yang, Z., Shao, J., 2019. Combustion characteristics and kinetics study of pulverized coal and semi-coke. High Temp. Mater. Process. 38, 783–791. https://doi.org/10.1515/htmp-2019-0034.
Yang, W., Wang, H., Zhang, M., Zhu, J., Zhou, J., Wu, S., 2016. Fuel properties and combustion kinetics of hydrochar prepared by hydrothermal carbonization of bamboo. Bioresour. Technol. 205, 199–204. https://doi.org/10.1016/j.biortech.2016.01.068.
Zhang, N., Wang, G., Zhang, J., Ning, X., Li, Y., Liang, W., Wang, C., 2020. Study on co-combustion characteristics of hydrochar and anthracite coal. J. Energy Inst. 93 (3), 1125–1137. https://doi.org/10.1016/j.joei.2019.10.006.
Zhang, X., Zhang, L., Li, A., 2017. Hydrothermal co-carbonization of sewage sludge and pinewood sawdust for nutrient-rich hydrochar production: Synergistic effects and products characterization. J. Environ. Manage. 201, 52–62. https://doi.org/10.1016/j.jenvman.2017.06.018.
Zhao, P., Shen, Y., Ge, S., Yoshikawa, K., 2014. Energy recycling from sewage sludge by producing solid biofuel with hydrothermal carbonization. Energy Convers. Manag. 78, 815–821. https://doi.org/10.1016/j.enconman.2013.11.026.